Sea ice thickness and recent Arctic warming

Lang, Andreas; Yang, Shuting; Kaas, Eigil

Published in:
Geophysical Research Letters

DOI:
10.1002/2016GL071274

Publication date:
2017

Document version
Publisher's PDF, also known as Version of record

AGU PUBLICATIONS

Geophysical Research Letters

RESEARCH LETTER
10.1002/2016GL071274

Sea ice thickness and recent Arctic warming

Andreas Lang[1,2], Shuting Yang[1], and Eigil Kaas[2]

[1]Danish Meteorological Institute, Copenhagen, Denmark, [2]Niels Bohr Institute, University of Copenhagen, Copenhagen, Denmark

Key Points:
- The recent sea ice thinning has significantly affected the Arctic climate
- Arctic sea ice thinning has significantly contributed to the recent Arctic amplification
- The inclusion of realistic ice thickness distribution in the model greatly improves the simulation of Arctic amplification

Supporting Information:
- Supporting Information S1
- Figure S1
- Figure S2
- Figure S3

Correspondence to:
S. Yang,
shuting@dmi.dk

Citation:
Lang, A., S. Yang, and E. Kaas (2017), Sea ice thickness and recent Arctic warming, *Geophys. Res. Lett.*, *44*, 409–418, doi:10.1002/2016GL071274.

Received 22 SEP 2016
Accepted 8 DEC 2016
Accepted article online 12 DEC 2016
Published online 13 JAN 2017

Abstract The climatic impact of increased Arctic sea ice loss has received growing attention in the last years. However, little focus has been set on the role of sea ice thickness, although it strongly determines surface heat fluxes. Here ensembles of simulations using the EC-Earth atmospheric model (Integrated Forecast System) are performed and analyzed to quantify the atmospheric impacts of Arctic sea ice thickness change since 1982 as revealed by the sea ice model assimilation Global Ice-Ocean Modeling and Assimilation System. Results show that the recent sea ice thinning has significantly affected the Arctic climate, while remote atmospheric responses are less pronounced owing to a high internal atmospheric variability. Locally, the sea ice thinning results in enhancement of near-surface warming of about 1°C per decade in winter, which is most pronounced over marginal sea ice areas with thin ice. This leads to an increase of the Arctic amplification factor by 37%.

1. Introduction

The Arctic's climate is changing rapidly, which is manifested in an unprecedented warming over the last century. Over the last 50 years, near-surface temperatures have risen more than twice as fast as the global average [*Serreze et al.*, 2009; *Screen and Simmonds*, 2010], a phenomenon termed "Arctic amplification." At the same time, the Arctic sea ice has experienced an extensive decline in both extent and thickness at an accelerating rate [*Stroeve et al.*, 2007; *Kwok and Untersteiner*, 2011]. While its extent has been monitored continuously at high resolution since the beginning of the satellite era in 1979, pan-Arctic thickness measurements only exist since the launch of NASAs Ice, Cloud, and land Elevation Satellite (ICESat) in 2003, and longer-term data sets rely on the combination of distinct in situ measurements. Yet one can reconstruct a thinning trend of especially inner multiyear ice over the last decades [*Kwok and Rothrock*, 2009; *Lindsay and Schweiger*, 2015].

While several processes have been proposed to contribute to this Arctic amplification, it is well established that the recent loss of sea ice plays an important role [e.g., *Screen and Simmonds*, 2010; *Doescher et al.*, 2012]: When ice melts, more dark open ocean with a lower albedo gets exposed, leading to more heat uptake by the ocean. Come autumn and winter, the excess heat gained in summer is subsequently released to the atmosphere, resulting in a warming of the atmosphere and hence less winter ice that will be more easily melted away next summer. This mechanism is referred to as albedo ice feedback and is related to sea ice extent. In addition, a second effect, the "insulation effect" [*Serreze and Barry*, 2011] is regulated by the ice's thickness: since sea ice insulates the ocean from a colder atmosphere, heat will try to travel upward via conduction against the temperature gradient. When the ocean releases heat back to the atmosphere in winter, thinner ice facilitates this heat transfer and hence warms the overlying air. These two effects lead to a time-lagged warming in response to sea ice loss.

Until now, studies investigating the response to recent sea ice changes mainly focused on the decline in extent, whereas—owing to a lack of comprehensive data—its thickness has received less attention and thus often kept fixed in atmosphere-only models. Yet with the sea ice having experienced substantial changes over large areas, studies using a fixed thickness miss a potentially important source of model skill and may hence underestimate the warming signal due to recent thinning of the Arctic sea ice, especially in winter when temperature gradients between ocean and atmosphere are greatest. Further, analyzing recent anomalously warm Arctic winters, *Overland and Wang* [2016] have suggested a link between sea ice thickness and large-scale circulation changes. Only a few atmospheric general circulation model (AGCM) studies investigating the atmospheric impact of sea ice singled out the role of sea ice thickness [e.g., *Gerdes*, 2006; *Rinke et al.*, 2006; *Krinner et al.*, 2010; *Semmler et al.*, 2016]. However, these are constrained to specific anomalous conditions;

to date, no modeling study using an AGCM has been conducted that assessed the longer-term transient atmospheric influence of changes in sea ice thickness only. The current study aims to quantify the impact of sea ice thickness on the atmosphere by using reanalysis ice thickness data as an estimate of the observed thinning to constrain the model.

2. Methods

2.1. Climate Model

We apply the atmospheric component of the global atmosphere-ocean-sea ice coupled climate model EC-Earth [*Hazeleger et al.*, 2012] v3.1, which is based on the numerical weather prediction model Integrated Forecast System (IFS) model version ifs-36r4, developed at the European Centre for Medium-Range Weather Forecast (ECMWF). The underlying model version's resolution is T255L91 (where "T" is the spectral resolution and "L" the number of model levels), corresponding to approximately 80 km in the horizontal, and 91 vertical levels, with a model top at 1 Pa (~75 km) [*European Centre for Medium-Range Weather Forecasts (ECMWF)*, 2010].

2.2. Sea Ice Parameterization

In the IFS, the ice slab has a standard thickness of 1.5 m and is discretized in four layers and five interfaces (original IFS layer distribution from top to bottom: 7 cm, 21 cm, 72 cm, and 50 cm); upper and lower boundary conditions are the net surface heat flux and the freezing point of sea water (−1.7°C), respectively. Heat conduction through sea ice follows a one-dimensional Fourier law of diffusion in (upward) z direction:

$$\left(\rho c_p\right) \cdot \frac{\partial T}{\partial t} = \frac{\partial}{\partial z}\left(\lambda \frac{\partial T}{\partial z}\right) = \frac{\partial F_C}{\partial z} \tag{1}$$

with temperature T, conductive heat flux F_C, the volumetric ice heat capacity $\rho c_p = 1.88 \cdot 10^6$ J m^{-3} K^{-1}, and the ice thermal conductivity $\lambda = 2.03$ W m^{-1} K^{-1}, which is solved using a tridiagonal matrix solver [*ECMWF*, 2010].

To account for the influence of realistic sea ice thickness changes, the above fixed ice depth and ice layers were relaxed to a daily varying ice thickness reanalysis data set with adaptive ice layers. This was done only for grid points containing sea ice, ensuring that all experiments use the same ice concentration. The thickness parameterization was modified in a way that the upper layer is always kept thin, as it is the most sensitive one for heat exchange. The new total sea ice thickness h_I is thus distributed into four layers $k_{1:4}$ using the following scheme:

1. For $h_I \leq 28$ cm: $k_{1:4} = 1/4 h_I$.
2. For 28 cm $< h_I \leq 1$ m: $k_1 = 7$ cm; $k_{2:4} = 1/3(h_I - k_1)$.
3. For $h_I > 1$ m: $k_1 = 7$ cm; $k_2 = 21$ cm; $k_3 = 72$ cm; $k_4 = h - \sum(k_{1:3})$.

In order to ensure a stable performance of the tridiagonal matrix solver, the minimum sea ice thickness h_I is set to 0.16 m.

2.3. Experimental Design

We conduct two sets of hindcast experiments comprising a 10-member ensemble (forced by different initial conditions from ERA-Interim reanalysis) that cover the period 1982–2013 and form part of the GREENICE AGCM experiments (see https://wiki.uib.no/greenice). The control run (hereafter *CTRL*) is forced by daily observed sea surface temperatures (SSTs) and sea ice concentration (SIC) from NOAA Optimum Interpolation [*Reynolds et al.*, 2007], and greenhouse gas (GHG) concentrations following CMIP5 protocol for the historical period until 2005 and RCP8.5 for the years since. Sea ice thickness is prescribed as a uniform slab of 1.5 m, as in the standard setup of the IFS. In order to investigate the atmospheric response to the sea ice thinning during the last three decades, a second set of experiments using a long-term thickness data set is employed (hereafter *RIT*). RIT uses the same forcing as CTRL except for the prescription of sea ice thickness, where the recent sea ice thinning is simulated using a daily updated thickness distribution. Since no "pure" observational data set of sea ice thickness is available until now that covers a longer time period and is spatially continuous, this study relies on reanalysis data from the Global Ice-Ocean Modeling and Assimilation System (GIOMAS) from the Polar Science Center, Washington [*Zhang and Rothrock*, 2003] to represent observed sea ice thickness. The reanalysis assimilates observed sea ice conditions (i.e., its concentration and drift) and SST (forced by National Centers for Environmental Prediction/National Center for Atmospheric Research reanalysis data)

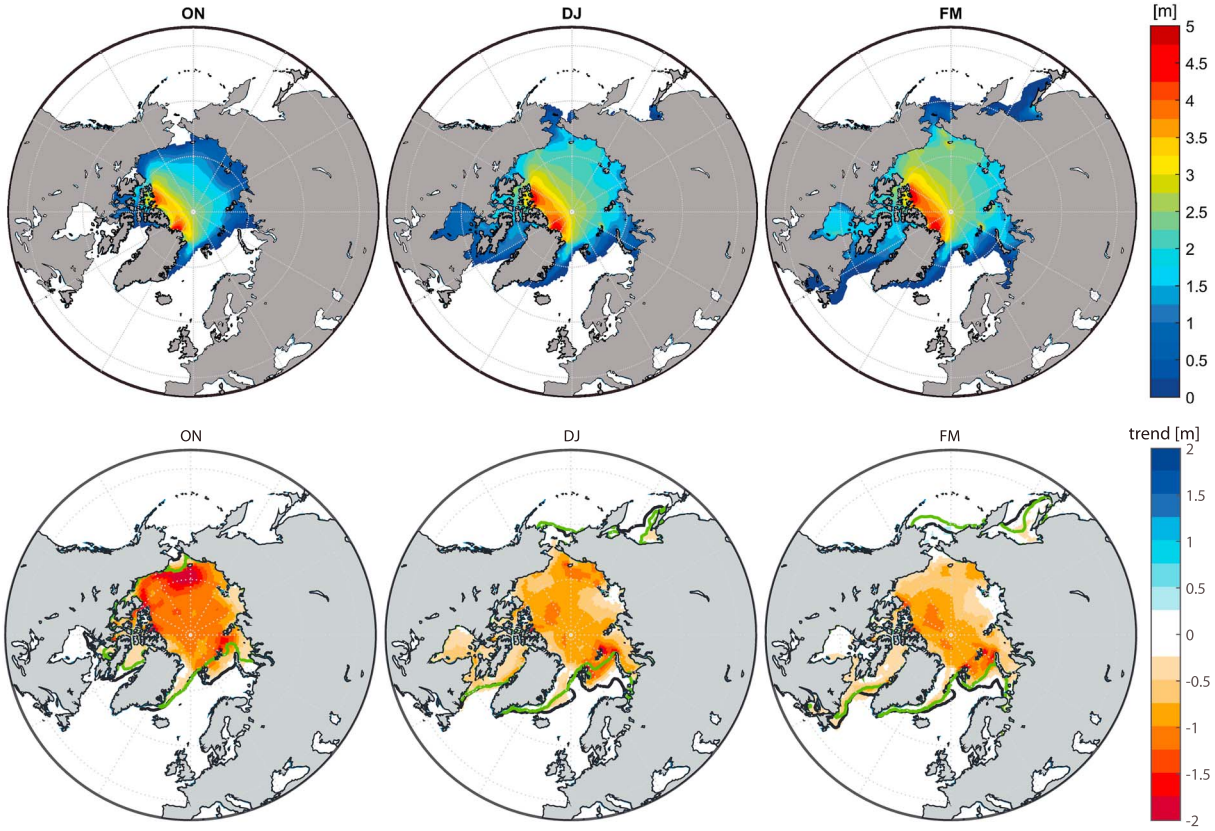

Figure 1. The 1982–2013 Arctic sea ice thickness: (top row) multiyear mean and (bottom row) change, for (left column) October–November, (middle column) December–January, and (right column) February–March after GIOMAS. Black (green) lines in Figure 1 (bottom row) represent the 1982 (2013) mean sea ice extent.

in a numerical model. The ice thickness is derived from the internal sea ice (thermo)dynamics, creating a continuous time series. The Northern Hemispheric version of this reanalysis set (PIOMAS) has been extensively evaluated against satellite, submarine, and in situ observations [e.g., *Schweiger et al.*, 2011; *Laxon et al.*, 2013; *Wang et al.*, 2016]. Despite some spatial bias in the ice thickness distribution, where the reanalysis tends to overestimate (underestimate) thin (thick) ice thickness, the estimates were found to agree well with observations. Yet the periods of the respective observational data sets are rather short, making a validation of GIOMAS long-term trend problematic. While satellite observations as well as in situ observations do endorse the long-term decrease in simulated Arctic sea ice thickness [*Laxon et al.*, 2013], the reconstructed thinning trend using observations is found to be even stronger than modeled in GIOMAS [*Schweiger et al.*, 2011; *Laxon et al.*, 2013], making the results of our study a conservative estimate. Despite the fact that GIOMAS is a model assimilation and thus constrained by the quality of assimilated observations, we consider GIOMAS to be the best available spatially and temporally extensive estimate of the actual long-term evolution of Arctic sea ice thickness. Figure 1 shows the multiyear mean thickness over the 1982–2013 period (top row) and the thickness change for the winter months during this period (bottom row) following GIOMAS. Arctic sea ice is thickest along the Canadian Archipelago and follows an annual cycle with maxima in March and minima in September. Over the last decades, sea ice thickness has been steadily decreasing in all seasons, especially that of the inner multiyear ice with reductions of up to 2 m since 1982.

Following *Screen et al.* [2013], we analyze 2 month periods instead of conventional seasons, because the thermal response to sea ice decline can exhibit temporal changes that may be averaged out on longer time scales. We limit our figures to the Northern Hemispheric winter (here October–March) results, since they have been shown to be more relevant for the impact of sea ice thickness [*Gerdes*, 2006; *Krinner et al.*, 2010], as temperature gradients between ocean and atmosphere are greatest. Statistical significance is tested using the Kolmogorov-Smirnov test (for RIT-CTRL) on the $\alpha = 95\%$ confidence level.

Table 1. Seasonal Cycle of Mean Arctic (70–90°N) Heat Flux Response (RIT-CTRL (W/m^2)) for Sensible Heat (SH), Latent Heat (LH), and Long-Wave Radiation (LW); the Root-Mean-Square Error (RMSE) of Both SAT Responses Respective to ERA-I and Bimonthly Arctic Amplification Factors (AAF) for ERA-Interim, CTRL, and RIT; and Their Relative Change Due To an Inclusion of Sea Ice Thickness[a]

	Energy Fluxes			SAT RMSE		AAF			
	SH	LH	LW	CTRL	RIT	ERA-I	CTRL	RIT	Change
Oct–Nov	0.11	0.15	0.57	0.51	0.23	6.6	4.2	5.4	29%
Dec–Jan	0.46	0.24	0.52	0.74	0.47	11.3	2.8	3.7	32%
Feb–Mar	0.11	0.08	0.40	0.52	0.22	6.9	1.6	3.1	94%
Apr–May	0.07	0.16	0.02	0.74	0.44	8.4	2.0	3.7	85%
Jun–Jul	0.04	0.11	0.01	0.07	0.05	1.3	1.1	1.3	19%
Aug–Sep	0.03	0.04	0.02	0.02	0.01	3.4	3.0	3.0	0%
Year	0.14	0.13	0.26	0.43	0.24	6.3	2.4	3.4	37%

[a]Response values as trends per decade; fluxes are defined positive upward.

3. Results

3.1. Energy Fluxes and Temperature

On average, surface turbulent and long-wave energy fluxes are directed upward in high latitudes, as the ocean loses energy to the colder atmosphere. Since sea ice works as an insulator, these upward heat fluxes are reduced over ice-covered areas. Table 1 shows the area-averaged pan-Arctic flux response to the recent thinning (RIT-CTRL) for the Arctic region, here defined as the area north of 70°N. Fluxes are defined positive upward. The response shows enhanced upward energy fluxes, both for turbulent heat (sensible + latent) as well as long-wave radiation. The strongest signal from sea ice thinning is seen throughout winter, when the temperature gradient between ocean and atmosphere is highest. The long-wave (turbulent heat) flux response peaks in early (middle) winter.

Figure 2 shows the ensemble mean surface air temperature (SAT) response to the recent evolution of sea ice conditions, SST, and GHGs since 1982 (RIT, middle row), the response to sea ice thinning (RIT-CTRL, bottom row), and the trend seen in the ERA-Interim reanalysis (top row). The signal in RIT shows that most regions of the Arctic Ocean have warmed; with up to 4°C per decade highest trends are found over the Eastern Arctic basin and the Barents-Kara Sea. Wintertime SAT trends over continents are much smaller than over the Arctic ocean. The general pattern and magnitude accord well with ERA-Interim, although it underestimates especially the Arctic midwinter warming, a feature potentially linked to the SIC data which show different trends then in ERA-Interim. The local December–January cooling over Siberia in ERA-Interim can be seen in individual ensemble members (see Figure S2 in the supporting information); yet the high internal variability masks this pattern in the ensemble mean.

How much of the modeled warming is due to the thinning of sea ice? The difference RIT-CTRL shows that prescribing a realistic sea ice thickness enhances warming trends locally by up to 1.5°C per decade over the Arctic Sea. As expected, the warming signal linked to sea ice thinning is most pronounced in winter and thus lags behind the time of strongest sea ice thinning, as the higher-temperature differences between ocean and atmosphere give rise to higher conductive heat fluxes and hence stronger surface heating. Comparing the spatial pattern with sea ice thickness changes (Figure 1) shows that strongest warming trends coincide with regions where the Arctic sea ice (i) has been declining most in extent and thickness *and* (ii) is relatively thin (i.e., in marginal ice areas). These regional warmings are congruent with a thickness loss of 1–2 m over the 32 year period. Apart from few minor remote relative cooling trends (weaker warming than in the control run, see, e.g., the Eastern U.S. in December–January, Figure 2, bottom row), no robust signals are found in lower latitudes. A comparison between RIT and RIT-CTRL shows that about a third to a half of the modeled wintertime warming over the Eastern Arctic Ocean is due to changes in ice thickness. On the other hand, sea ice thinning contributes only little to the regionally strongest warming in the Barents Sea. This is likely due to the relatively strong impact of ice extent reductions and the comparatively small change in ice thickness due to predominantly seasonal ice in this area. Linking the SAT response with the heat flux response stresses that the temperature signal is primarily of thermodynamic nature rather than forced via the large-scale circulation.

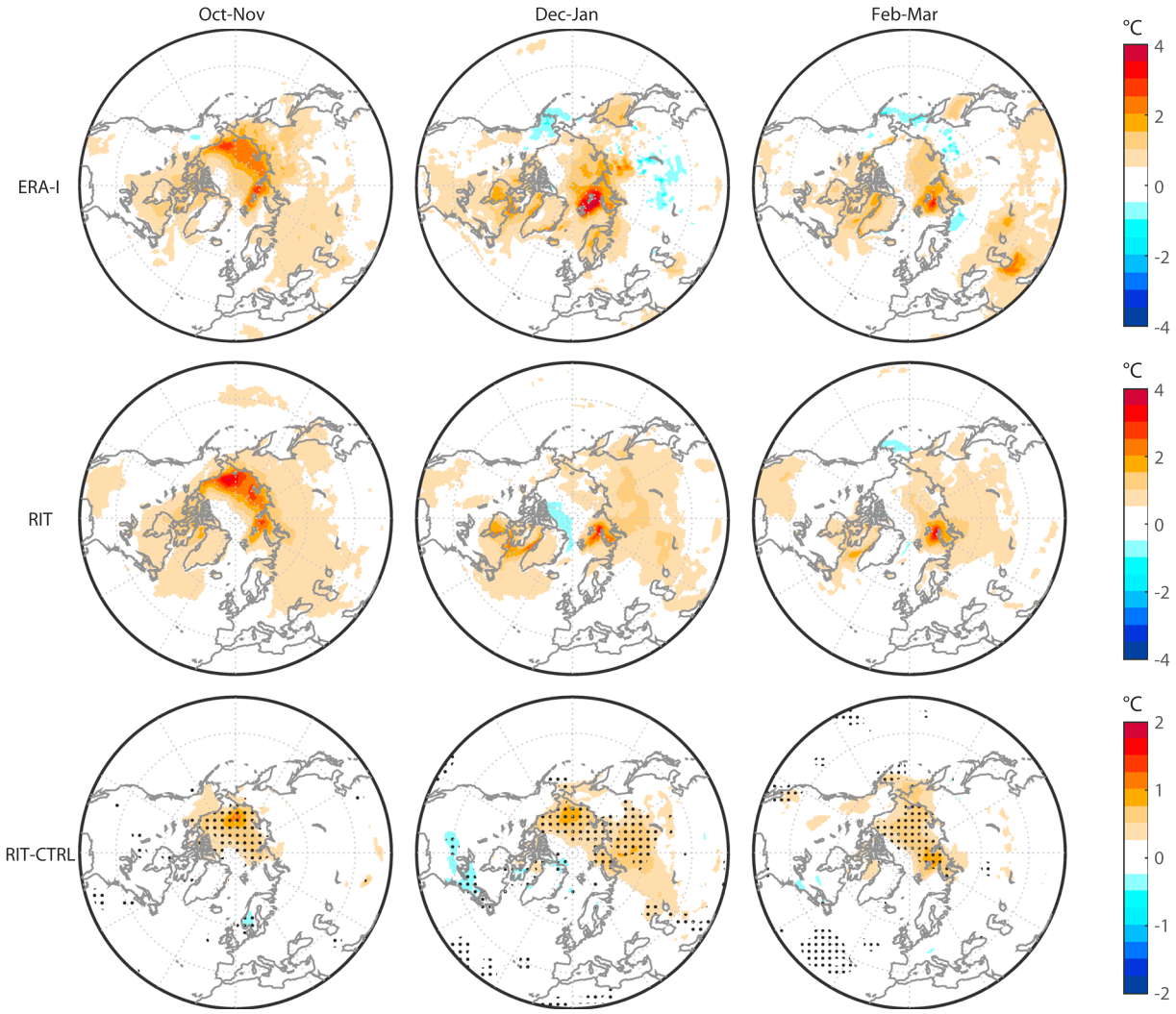

Figure 2. Surface Air temperature response for (top row) ERA-I, (middle row) RIT, and (bottom row) RIT-CTRL, shown as trends per decade (°C). Hatching in RIT-CTRL indicates areas significant on the 95% confidence level. Note the different color scales.

The enhanced warming due to an inclusion of a variable thickness generally leads to a better match with ERA-Interim and thus increases the IFS' model skill (see Table 1).

The vertical profile of Arctic warming has received much attention concerning the debate about the drivers of Arctic amplification, as it can give insights into the role of different mechanisms through their respective "fingerprints" [*Screen et al.*, 2010]. The total response to sea ice, SST, and GHG forcing (RIT; Figure 3, middle row) shows the well-known structure of Arctic amplification: strongest warming is found in the lowermost troposphere up to 850 hPa (a result of the stably stratified boundary layer in the Arctic) at roughly 70–80°N, i.e., the latitudes where sea ice reduced most in extent and thickness. The spatial pattern stresses the role of sea ice in the surface-based Arctic amplification. ERA-Interim (Figure 3, top row) shows a similar pattern as seen in RIT but with overall stronger warming trends. The position of strongest modeled warming is shifted farther south in RIT, a feature related to the absence of Siberian wintertime cooling (see Figure 2). However, there is considerable uncertainty in the validity of the Arctic vertical temperature profile as seen in reanalysis sets like ERA-Interim, and different sets can give different results (as, e.g., in *Graversen et al.* [2008] and *Screen and Simmonds* [2010]). The response to a realistic sea ice thinning (RIT-CTRL; Figure 3, bottom row) shows a significant warming of near-surface layers only up to 950 hPa and latitudes north of 70°N, congruent with regions of sea ice thinning. That is, changes in sea ice thickness only affect lower levels of the troposphere and response signals quickly vanish with height. This supports the understanding that sea ice loss is linked to surface-based warming [*Kumar et al.*, 2010; *Screen et al.*, 2013], while the Arctic amplification in the free

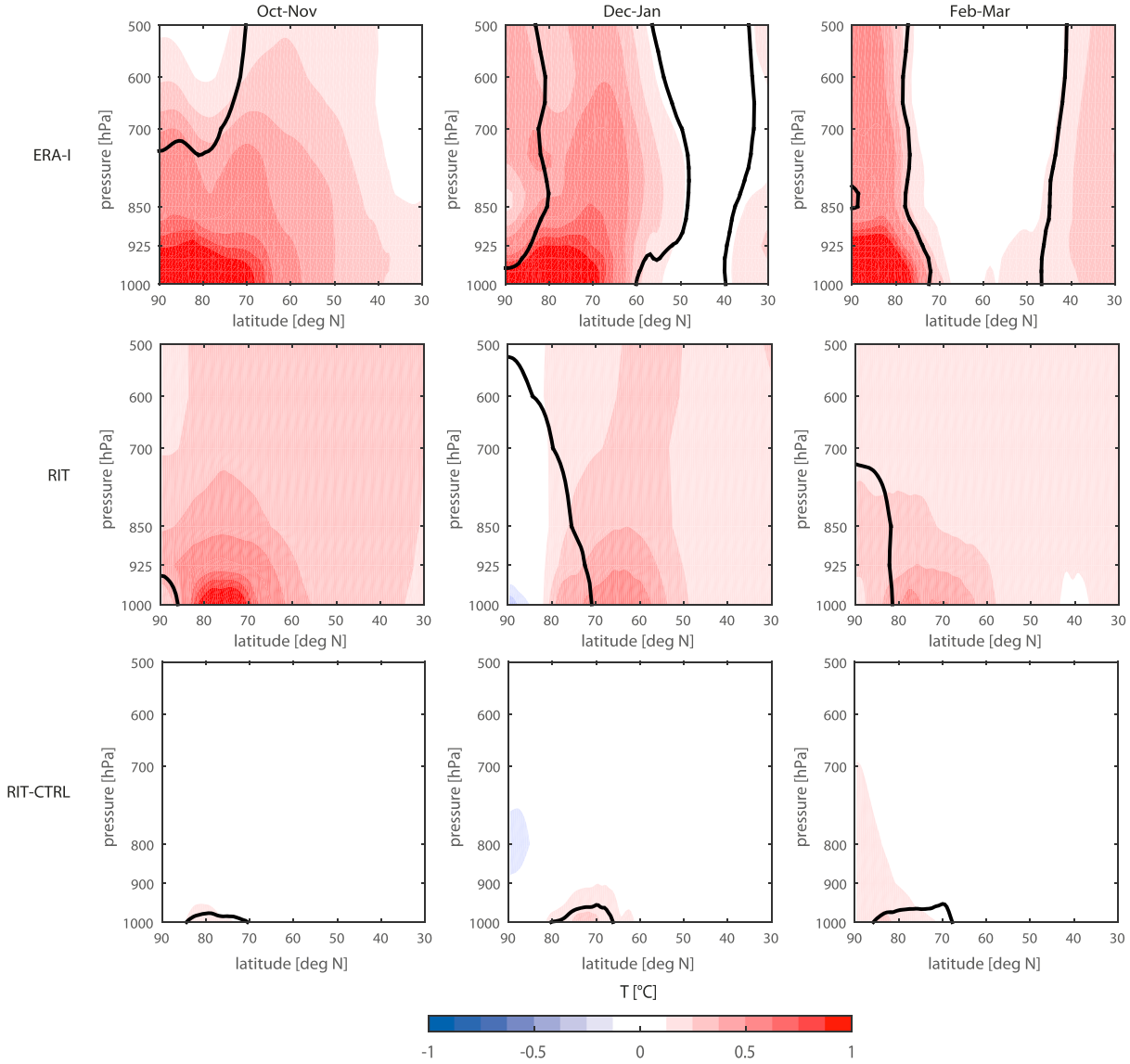

Figure 3. Vertical profile of temperature response for (top row) ERA-I, (middle row) RIT, and (bottom row) RIT-CTRL, shown as trends per decade (°C). Contour lines indicate areas significant on the 95% confidence level.

atmosphere cannot directly be linked to sea ice loss, even if the recent sea ice thinning is considered. This stresses that there are likely still other processes involved.

To set the local warming response due to sea ice thinning in context with the recent Arctic amplification, we compare Arctic amplification factors (AAF) between RIT and CTRL, calculated as the SAT trend in the Arctic region (70°N–90°N) divided by the global mean trend. As seen in Table 1, CTRL underestimates the AAF, especially in winter, a feature many CMIP3 models exhibit [*Mahlstein and Knutti*, 2012]. In our case this mainly stems from larger (smaller) global (Arctic) SAT trends in IFS compared to ERA-Interim. However, reanalysis sets such as ERA-Interim may be afflicted with systematic errors due to the lack of in situ observations and the handling of sea ice data and hence tend to shift toward their own climate. The inclusion of realistic ice thickness distribution greatly improves the simulation of AAF and leads to an increase in the year-round AAF over the last 32 years by 37% from 2.45 to 3.36, which can mainly be attributed to the enhanced winter warming. The strongest relative impact of sea ice thinning on recent Arctic amplification is found in late winter (AAF increase by 94%), while the total modeled Arctic amplification is strongest in early winter. Hence, the recent Arctic sea ice thinning has significantly contributed to and amplified the surface-based Arctic amplification.

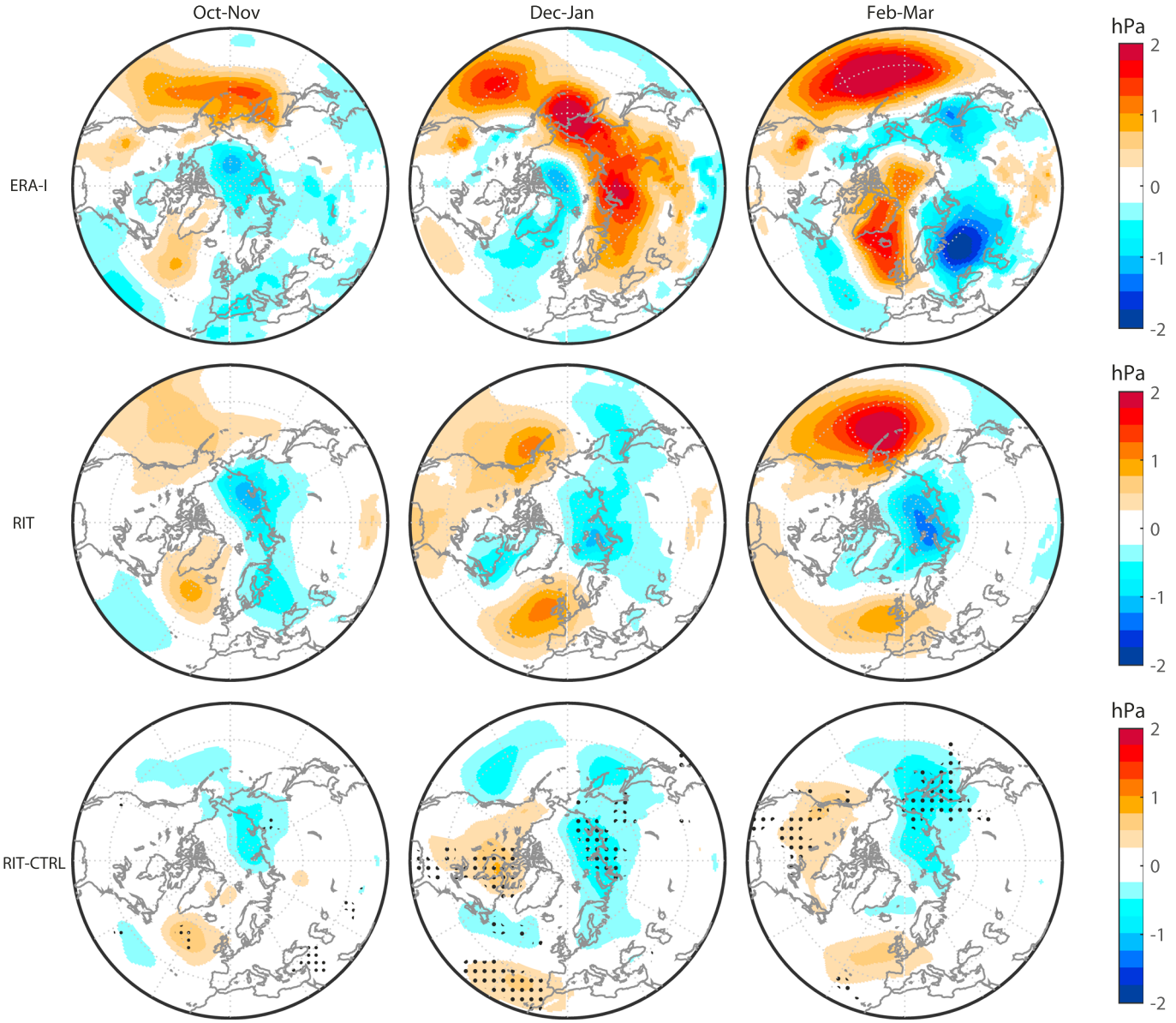

Figure 4. Same as Figure 2 but for SLP.

3.2. Large-Scale Circulation

The local energy flux response to sea ice thinning shown above acts as a forcing for the atmospheric circulation and is thus expected to affect remote mass and wind fields. RIT (Figure 4, middle row) shows a dipole pattern of reduced (increased) SLP in the Arctic (over Atlantic and Pacific Oceans) throughout winter, indicating a weakening of the Icelandic and Aleutian Lows. The negative trends in the Arctic are especially evident over the Laptev, East Siberian, and Kara Seas, exhibiting small but significant trends of −1 to −2 hPa per decade. With 2–3 hPa per decade, positive SLP trends are strongest in February–March over the North Pacific. The SLP decrease over the Arctic Sea is also detectable in ERA-Interim (Figure 4, top row), although only in early winter. The ERA-Interim trend in December–January with a strengthening of the Siberian High is not seen in the RIT ensemble mean. However, there is a large spread among the response patterns. In fact, one of the RIT members exhibits a similar positive response of the Siberian High as in ERA-Interim (see Figure S3); yet a large internal variability masks this feature.

The response to the recent sea ice thinning (RIT-CTRL; Figure 4, bottom row) shows a weak dipole of lower (higher) SLP over the Eastern Arctic Sea (Northeast Atlantic and North America), especially in middle and late

winter; the October–November response is less pronounced. The spatial pattern of the negative SLP response to the recent sea ice thinning is congruent with the location of strongest warming over marginal sea ice areas of the Eastern Arctic Sea. Since both RIT and RIT-CTRL show similar patterns over the Arctic basin and the Atlantic, the recent sea ice thinning has clearly contributed to the RIT-modeled SLP trends, accounting for roughly half of the detected trend strength during 1982–2013. However, the few areas with significance on the 95% confidence level and a large spread between individual ensemble members stress the high internal atmospheric variability. Reduced SLP might further impact the large-scale circulation, inducing remotely forced temperature anomalies in the Arctic. *Nakamura et al.* [2016b] documented a negative Arctic Oscillation (AO) in response to reduced sea ice conditions. Yet we find large variability in RIT response patterns in February–March. Both negative and positive AO-like patterns can be seen in the individual members (see Figure S3). Negative AO patterns have been associated with enhanced Arctic warming as well as anomalously cold winters in midlatitudes due to a stronger meandering of the flow and a resulting increase in meridional heat transport into the Arctic [e.g., *Nakamura et al.*, 2016b]. The absence of this unique feature in our simulations suggests that the enhanced Arctic warming found in this study does not result from meridional heat transport induced by large-scale circulation changes but rather stem from a local thermodynamic forcing. However, nonlinear behavior of sea ice-AO interactions has been suggested [*Petoukhov and Semenov*, 2010], as well as a high sensitivity of the spatial pattern of sea ice forcing [*Pedersen et al.*, 2015], which could explain the lack of AO signal in our simulations. In the study by *Nakamura et al.* [2016a] it was concluded that the negative AO response to Arctic sea ice reduction involves stratosphere-troposphere couplings via wave mean flow interactions. They used a set of specially designed numerical experiments in a high-top AGCM with 56 vertical levels and model top around 60 km. It is unclear why we obtain a rather different result using IFS in our configuration, which also has a good representation of stratospheric dynamics. This will be the subject of a future study. The RIT-CTRL SLP response pattern does not indicate any resemblance to the leading atmospheric modes, which is consistent with *Screen et al.* [2013] who examined the response to realistic changes in sea ice concentration over the same period. This suggests that the simulated circulation response and its interaction with atmospheric modes are relatively small in comparison to natural variability, stressing the wide model spread between ensemble members and suggesting that such circulation patterns are mainly internally driven and do not necessarily depend on a remote forcing. In turn, this emphasizes the importance of large ensembles to obtaining robust results. The February–March RIT-CTRL response with troughing over the Aleutian Islands and ridging over northwestern North America, however, is similar to the event of winter 2016, where these pressure anomalies worked to split the tropospheric polar vortex over the Arctic and led to an anomalously warm Arctic [*Overland and Wang*, 2016].

4. Discussion and Conclusion

This study has investigated the atmospheric impact of the recent Arctic sea ice thinning since 1982. The results show that with an inclusion of sea ice thickness in the model, it is possible to better simulate the Arctic amplification. Thinner sea ice has a clear local thermodynamic effect as it gives rise to significantly enhanced upward heat fluxes and thus elevated temperatures. The enhanced wintertime warming of around 1°C per decade is mainly found over areas of sea ice thinning where the ice is already thin, i.e., mostly in marginal ice areas. In contrast, regions of thick ice do not exhibit significant signals. Temperature changes beyond the Arctic basin are absent due to a high internal atmospheric variability in lower latitudes. The SLP response is negative locally, showing small lowering trends in response to the observed ice thinning over the last decades, and positive over some areas off the ice edge.

Overall, the impact of recent sea ice thinning is less pronounced than that due to a decline in extent (as, e.g., in *Screen et al.* [2013]). Yet sea ice thinning has had a considerable impact on the local Arctic near-surface temperature trends over the last decades and significantly contributed to the Arctic amplification, raising the AAF by 37% compared to the control run, predominantly due to the enhanced late-winter warming with thinning ice. Hence, sea ice loss might be a stronger driver of Arctic amplification than previously assumed. The temperature response to the recent thinning is confined to near-surface layers and thus strengthens the view that sea ice accounts for most of the surface-based Arctic warming. Yet sea ice changes are most likely not the only driver of Arctic amplification; in addition, other feedbacks such as cloud, water vapor, or temperature feedbacks likely play a role and may complement one another. Locally, sea ice thickness clearly affects temperatures and should be accurately represented in climate models addressing recent and future climate, especially in winter and in the marginal ice area. However, due to the high atmospheric internal variability (AIV),

especially concerning more dynamical quantities such as SLP, these local anomalies are unable to induce significant responses in midlatitudes via the atmospheric circulation: With growing distance from the forcing source the signal to noise ratio decreases, leaving AIV as the most important predictor of the large-scale circulation.

Since sea ice thickness changes mostly matter in areas of thin winter ice, an ongoing thinning will enhance the modeled climatic trends in the future. A locally increased surface warming due to thinner ice will further boost Arctic amplification, as this positive feedback strengthens. Reduced SLP might impact the large-scale circulation, also inducing remotely forced temperature anomalies in the Arctic, e.g., by breaking the polar vortex [*Overland and Wang*, 2016]. Hence, a realistic sea ice thickness distribution should be incorporated in model experiments; it improves model skill, especially concerning local winter climate and Arctic amplification.

However, a major caveat of this study's underlying model lies in the sea ice parameterization: The IFS does not account for snow accumulation on top of the ice. Yet it does theoretically affect the heat exchange, as snow is a strong insulator. Hence, the model likely overestimates the absolute heat fluxes through the ice slab, although potential feedbacks between sea ice changes and snowfall could further complicate the situation, leaving the total combined effect uncertain.

Additional experiments using an idealistically reduced sea ice thickness (see supporting information) can further investigate the response to a more drastic and widespread thinning and shed light on a potential nonlinear response of the large-scale circulation, as, e.g., found in *Petoukhov and Semenov* [2010]. Preliminary results indeed indicate such a nonlinearity as the SLP shows a distinct response than seen in RIT.

The reanalysis thickness used here may not be equated with actual observations; unless longer spatially consistent observational data sets are available, one relies on model assimilation to represent the actual trend. Hence, our quantitative results are constrained by the validity of the reanalysis data set. However, assuming that GIOMAS reasonably reproduces the actual development of Arctic sea ice thickness, this study has provided a first estimate about the magnitude of recent Arctic warming that may attribute to sea ice thinning. If any, GIOMAS rather conservative estimate of the thinning trend compared to observations [*Schweiger et al.*, 2011; *Laxon et al.*, 2013] suggests that the atmospheric impact of the recent Arctic sea ice thinning could be even stronger. A better understanding of the processes linking sea ice and the atmosphere will not only improve our knowledge of the climate system but also enhance model predictability, thus potentially entailing societal benefits.

Acknowledgments
This work was supported by the NordForsk project GREENICE (grant 61841) and the European Research Council under the European Community's Seventh Framework Programme (FP7/2007-2013)/ERC grant agreement 610055 as part of the ice2ice project. The GIOMAS sea ice thickness data are available publicly through http://psc.apl.washington.edu/zhang/Global_seaice/data.html. We thank Editor J. Stroeve and two anonymous reviewers for their constructive comments.

References

Doescher, R., T. Vihma, and E. Maksimovich (2012), Recent advances in understanding the Arctic climate system state and change from a sea ice perspective: A review, *Atmos. Chem. Phys.*, *14*(24), 13,571–13,600, doi:10.5194/acp-14-13571-2014.

European Centre for Medium-Range Weather Forecasts (ECMWF) (2010), IFS documentation–CY36r1. part IV: physical processes. [Available at http://www.ecmwf.int/sites/default/files/elibrary/2010/9233-part-iv-physical-processes.pdf, accessed 11.07.2016.]

Gerdes, R. (2006), Atmospheric response to changes in Arctic sea ice thickness, *Geophys. Res. Lett.*, *33*, L18709, doi:10.1029/2006GL027146.

Graversen, R. G., T. Mauritsen, M. Tjernström, E. Källén, and G. Svensson (2008), Vertical structure of recent Arctic warming, *Nature*, *451*(7174), 53–56, doi:10.1038/nature06502.

Hazeleger, W., et al. (2012), EC-Earth V2. 2: Description and validation of a new seamless earth system prediction model, *Clim. Dyn.*, *39*(11), 2611–2629, doi:10.1007/s00382-011-1228-5.

Krinner, G., A. Rinke, K. Dethloff, and I. V. Gorodetskaya (2010), Impact of prescribed Arctic sea ice thickness in simulations of the present and future climate, *Clim. Dyn.*, *35*(4), 619–633, doi:10.1007/s00382-009-0587-7.

Kwok, R., and D. A. Rothrock (2009), Decline in Arctic sea ice thickness from submarine and ICESat records: 1958–2008, *Geophys. Res. Lett.*, *36*, L15501, doi:10.1029/2009GL039035.

Kwok, R., and N. Untersteiner (2011), The thinning of Arctic sea ice, *Phys. Today*, *64*(4), 36–41.

Kumar, A., J. Perlwitz, J. Eischeid, X. Quan, T. Xu, T. Zhang, M. Hoerling, B. Jha, and W. Wang (2010), Contribution of sea ice loss to Arctic amplification, *Geophys. Res. Lett.*, *37*, L21701, doi:10.1029/2010GL045022.

Laxon, S. W., et al. (2013), CryoSat-2 estimates of Arctic sea ice thickness and volume, *Geophys. Res. Lett.*, *40*, 732–737, doi:10.1002/grl.50193.

Lindsay, R. W., and A. Schweiger (2015), Arctic sea ice thickness loss determined using subsurface, aircraft, and satellite observations, *Cryosphere*, *9*, 269–283, doi:10.5194/tc-9-269-2015.

Mahlstein, I., and R. Knutti (2012), September Arctic sea ice predicted to disappear near 2°C global warming above present, *J. Geophys. Res.*, *117*, D06104, doi:10.1029/2011JD016709.

Nakamura, T., K. Yamazaki, K. Iwamoto, M. Honda, Y. Miyoshi, Y. Ogawa, Y. Tomikawa, and J. Ukita (2016a), The stratospheric pathway for Arctic impacts on midlatitude climate, *Geophys. Res. Lett.*, *43*(7), 3494–3501, doi:10.1002/2016GL068330.

Nakamura, T., K. Yamazaki, M. Honda, J. Ukita, R. Jaiser, D. Handorf, and K. Dethloff (2016b), On the atmospheric response experiment to a Blue Arctic Ocean, *Geophys. Res. Lett.*, *43*, 394–402, doi:10.1002/2016GL070526.

Overland, J. E., and M. Wang (2016), Recent extreme arctic temperatures are due to a split polar vortex, *J. Clim.*, *29*(15), 5609–5616, doi:10.1175/JCLI-D-16-0320.1.

Pedersen, R. A., I. Cvijanovic, P. L. Langen, and B. M. Vinther (2015), The impact of regional arctic sea ice loss on atmospheric circulation and the NAO, *J. Clim.*, *29*(2), 889–902, doi:10.1175/JCLI-D-15-0315.1.

Petoukhov, V., and A. S. Semenov (2010), A link between reduced Barents-Kara sea ice and cold winter extremes over northern continents, *J. Geophys. Res.*, *115*, D21111, doi:10.1029/2009JD013568.

Reynolds, R. W., T. M. Smith, C. Liu, D. B. Chelton, K. S. Casey, and M. G. Schlax (2007), Daily high-resolution-blended analyses for sea surface temperature, *J. Clim.*, *20*(22), 5473–5496, doi:10.1175/2007JCLI1824.1.

Rinke, A., W. Maslowski, K. Dethloff, and J. Clement (2006), Influence of sea ice on the atmosphere: A study with an Arctic atmospheric regional climate model, *J. Geophys. Res.*, *111*, D16103, doi:10.1029/2005JD006957.

Schweiger, A., R. Lindsay, J. Zhang, M. Steele, H. Stern, and R. Kwok (2011), Uncertainty in modeled Arctic sea ice volume, *J. Geophys. Res.*, *116*, C00D06, doi:10.1029/2011JC007084.

Screen, J. A., and I. Simmonds (2010), The central role of diminishing sea ice in recent Arctic temperature amplification, *Nature*, *464*(7293), 1334–1337, doi:10.1038/nature09051.

Screen, J. A., C. Deser, and I. Simmonds (2010), Local and remote controls on observed Arctic warming, *Geophys. Res. Lett.*, *39*, L10709, doi:10.1029/2012GL051598.

Screen, J. A., I. Simmonds, C. Deser, and R. Tomas (2013), The atmospheric response to three decades of observed Arctic sea ice loss, *J. Clim.*, *26*(4), 1230–1248, doi:10.1175/JCLI-D-12-00063.1.

Semmler, T., T. Jung, and S. Serrar (2016), Fast atmospheric response to a sudden thinning of Arctic sea ice, *Clim. Dyn.*, *46*(3), 1015–1025, doi:10.1007/s00382-015-2629-7.

Serreze, M. C., A. P. Barrett, J. C. Stroeve, D. N. Kindig, and M. Holland (2009), The emergence of surface-based Arctic amplification, *Cryosphere*, *3*(1), 11–19, doi:10.5194/tc-3-11-2009.

Serreze, M. C., and R. G. Barry (2011), Processes and impacts of Arctic amplification: A research synthesis, *Global Planet. Change*, *77*(1), 85–96, doi:10.1016/j.gloplacha.2011.03.004.

Stroeve, J., M. Holland, W. Meier, T. Scambos, and M. Serreze (2007), Arctic sea ice decline: Faster than forecast, *Geophys. Res. Lett.*, *34*, L09501, doi:10.1029/2007GL029703.

Wang, X., J. Key, R. Kwok, and J. Zhang (2016), Comparison of Arctic sea ice thickness from satellites, aircraft, and PIOMAS data, *Remote Sens.*, *8*(9), 713, doi:10.3390/rs8090713.

Zhang, J., and D. A. Rothrock (2003), Modeling global sea ice with a thickness and enthalpy distribution model in generalized curvilinear coordinates, *Mon. Weather Rev.*, *131*(5), 845–861, doi:10.1175/1520-0493(2003)131<0845:MGSIWA>2.0.CO;2.